Fachtagung "Lasermethoden in der Strömungsmesstechnik"
8. – 10. September 2015, Dresden

Thermographic Particle Image Velocimetry

Thermographic Particle Image Velocimetry

Christopher Abram[1], Benoit Fond[2] and Frank Beyrau[1]
[1] Lehrstuhl für Technische Thermodynamik, Otto-von-Guericke-Universität Magdeburg, 39104 Magdeburg, Germany
[2] Department of Mechanical Engineering, Imperial College London, London SW7 2AZ, United Kingdom

Key words: Thermometry, Velocimetry, Thermographic Phosphors, Heat Transfer

Summary

This work describes a novel technique for simultaneous time-resolved temperature and velocity imaging in fluids based on thermographic phosphor particles. Thermographic phosphors are solid materials doped with optically active ions, with luminescence properties that can be exploited for remote thermometry. For thermographic PIV, micron-sized phosphor particles are seeded into the flow as a tracer. Since the particles are so small, their motion and temperature rapidly assume that of the surrounding gas. The flow velocity is determined using a conventional PIV approach while the temperature is determined from the temperature dependent phosphorescence emission spectrum after excitation by an additional UV laser. Two spectrally filtered images are recorded and a ratio-based method is used to determine the particle temperature. High-speed measurements at 3kHz repetition rate are demonstrated in the wake of a heated cylinder.

Introduction

Turbulent flows involving heat transfer and chemical reactions play a central role in a wide range of heating, transportation and power-generation devices. The behavior of such flows is governed by complex interactions between heat transfer, mixing, reaction chemistry, and the turbulent flow field. Improved understanding of the underlying phenomena necessitates simultaneous scalar-velocity measurements with appropriate resolution in space and time. High-speed (kHz repetition rates) planar measurements, in particular, can provide valuable insight into the transient nature of these instabilities as well as datasets that challenge the results of numerical simulations.
However, obtaining such measurements is difficult. For the well-established particle image velocimetry (PIV) technique, tracer particles must be seeded into the flow, which strongly interfere with classic scalar imaging techniques such as Rayleigh or Raman scattering. In addition, the application of existing high-speed scalar measurement techniques is often not possible due to the comparatively low pulse energies offered by current laser technology. A versatile technique that overcomes these challenges is still required.
In recent years, single-shot simultaneous temperature and velocity imaging has been demonstrated at low repetition rates using a combined phosphor thermometry and PIV technique (see e.g. Fond et al. 2012 and references therein). "Thermographic PIV" is based on thermographic phosphors, which are solid materials with luminescence properties that can

be exploited for remote thermometry. Micrometer-sized phosphor particles are seeded into fluid flows and used as a tracer. Velocimetry is performed with a conventional PIV approach, using the Mie scattered light from the phosphor particles. Following simultaneous UV excitation, these particles emit phosphorescence with a temperature dependent emission spectrum. When two spectrally filtered images of the particle phosphorescence emission are recorded, the tracer temperature can be determined using a ratio-based method. The diameter of the particles is carefully chosen so that their velocity and temperature rapidly assume that of the surrounding gas.

This technique has several important advantages. The tracer materials are chemically inert and have a high melting point (>2000 K), and for many phosphors the emission is insensitive to pressure and oxygen quenching, making them particularly suitable for reactive flow applications. In addition, many thermographic phosphors have relatively broad excitation spectra allowing direct excitation with solid-state lasers, and their subsequent emission is often in the visible range, permitting the use of non-intensified cameras.

There is a wide variety of thermographic phosphors with very different optical characteristics, and reported applications of gas-phase phosphor thermometry have employed different phosphors as a tracer material (e.g. Omrane et al. 2008; Fond et al. 2012; Jenkins et al. 2012; Rothamer and Jordan 2012; Jordan and Rothamer 2013). A method for characterizing the luminescence of particles dispersed in fluids is described in (Fond et al. 2015).

The authors have previously used the phosphor $BaMgAl_{10}O_{17}:Eu^{2+}$ (BAM:Eu), which has a short phosphorescence lifetime of 1 µs and a high quantum efficiency. These are important features that allow reasonable signal levels from particles dispersed in the gas-phase, where the integration (exposure) time of the measurement is limited and the particles must be small enough to accurately trace turbulent flow fluctuations, restricting the number of luminescent centres in the measurement probe volume. It has been shown previously for this phosphor, at low repetition rates (5 Hz), that even at fluences of a few mJ/cm^2 enough signal for precise single shot temperature measurements can be collected (Fond at al. 2012).The frequency-tripled output of DPSS lasers, on the order of a few mJ, is sufficient to saturate this phosphor using light sheets a few hundred micrometres thick that are typically used in laser-based imaging experiments. Therefore, signal levels are not limited by the low pulse energies of high-speed lasers and the possibility of kHz rate thermometry and velocimetry arises. Accordingly, here we present a high-speed measurement technique based on seeded BAM:Eu phosphor particles for simultaneous temperature and velocity imaging in turbulent gas flows. The single shot pixel-to-pixel precision of the temperature imaging technique at kHz repetition rates is assessed in a turbulent heated jet. The combined diagnostics are used to investigate unsteady heat transfer behind a heated cylinder in a cross flow, where time-resolved measurements of the temperature and velocity fields are presented.

Experiment

Initial measurements were performed in an electrically heated jet of air (21 mm diameter, velocity of 7 m/s) surrounded by a room temperature co-flow (80 mm diameter, velocity of 0.5 m/s) in order to assess the precision and accuracy of the technique. In the second heat transfer study, the central nozzle was removed and a pipe of 6.25 mm diameter heated to 530 K was positioned horizontally above the co-flow as shown in Fig. 1. The free stream velocity was set to 1.6 m/s so at a temperature of 293 K the Reynolds number was around 700, resulting in irregular vortex shedding in the wake of the cylinder (Williamson 1996).

For flow measurements based on solid tracer particles, the particle temperature and velocity should match that of the gas. The technique indirectly determines the gas properties by measuring the movement and luminescent properties of seeded phosphor particles. Consequently the measurement accuracy relies on how rapidly the tracer particles adjust to changes in gas temperature and velocity. For micrometer-sized particles, the Reynolds number is

below unity for a wide range of gas viscosities and slip velocities, and a Stokes flow can be assumed. Considering a step change in gas velocity, the slip between the particle and the gas decays exponentially and can be characterized using the particle relaxation time constant (see Raffel et al 2007):

$$\tau_u = d_p^2 \frac{\rho_p}{18\mu_g}$$

where ρ is the density, μ the dynamic gas viscosity and d the particle diameter, with subscripts p and g referring to the properties of the particle and gas, respectively. The relaxation time scales with the square of the particle diameter. It also increases with decreasing gas temperature owing to the decrease in viscosity, and scales with the tracer material density. Most phosphor materials such as BAM:Eu (3.70 g/cm3) have a density similar to tracers widely used in PIV such as TiO_2 (4.23 g/cm3) and Al_2O_3 (3.94 g/cm3), resulting in very similar response times. The 3τ (95%) relaxation times for 2 μm particles is around 50 μs at a mean temperature of 1150 K. If faster response times are needed for a particular experiment, smaller particles may be required (Picano et al 2011).
The thermometry technique assumes thermal equilibrium between gas and particles, so that the gas temperature can be inferred from the temperature-dependent emission properties of the phosphor. For example across a flame front, the gas temperature rapidly increases due to the reaction heat release. However, owing to the volumetric heat capacity of the particle, a large transfer of thermal energy through the poorly conductive gas is required in order to achieve thermal equilibrium. Consequently, an analysis of the particle temperature response is necessary before applying the technique for turbulent flow diagnostics. Assuming the tracer particles follow the flow, heat transfer to the particle is solely by conduction. A simple lumped capacitance heat transfer model was used to simulate the response of spherical particles. The particle thermal conductivity k_p, of the order 10 - 20 W/mK for some well characterized host materials such as YAG or Y_2O_3 (Klein and Croft 1967), is several orders of magnitude larger than the gas conductivity and so the temperature inside the sphere can be considered uniform at all times. Using the Nusselt relation for heat transfer by conduction from a spherical surface to a stationary, infinite medium around the surface, one can derive an expression for the particle relaxation time:

$$\tau_T \approx d_p^2 \frac{\rho_p C_p}{12 k_g}$$

In both test cases presented here, the gas streams were seeded with 2 μm BAM:Eu phosphor particles using reverse cyclone seeders. For these particles, the above equation yields 3τ (95%) temperature relaxation times very similar to the velocity relaxation times (around 40 μs at 1150 K).
Figure 1 shows the experimental setup for high-speed thermographic PIV. For thermometry, the phosphor particles were excited using the third harmonic of a diode pumped Nd:YAG laser with a pulse duration of 25 ns and a pulse energy of 1.3 mJ at 3 kHz. The beam was expanded using a Galilean telescope and then formed into a 600 μm thick and 50 mm high light sheet using cylindrical lenses. The phosphorescence emission was detected by two non-intensified high-speed CMOS cameras (12 bit, 1024 x 1024 pixels), fitted with 50 mm f/1.4 lenses. The cameras were operated at 3 kHz with an exposure time of 9 μs. However, the actual measurement duration is determined by the phosphorescence decay time of BAM:Eu (1 μs at room temperature). A long pass dichroic 45° beamsplitter and two interference filters (466-40 nm and 420-30 nm) were used to separate and filter the two detection channels, as shown in Fig. 2. The entire camera/beamsplitter system was aligned using micrometer stages to minimize relative distortion and differences in light collection path.

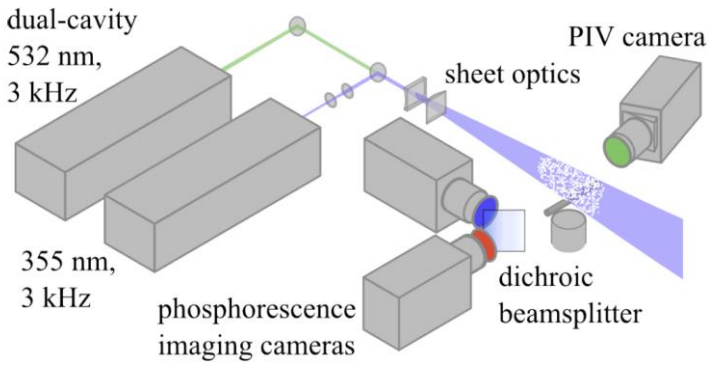

Fig. 1: Experimental setup for high-speed thermographic particle image velocimetry.

After acquisition, background images were recorded and subtracted from the image pairs. Images were then spatially overlapped using software-based mapping based on images of a calibration target. A cutoff filter at 15 counts was applied (corresponding to three times the readout noise of the camera), followed by 4 x 4 digital binning and a 3 x 3 unweighted moving average filter. The final spatial resolution was 720 µm, experimentally determined by the full width half maximum of the line spread function measured using a scanning edge technique. A ratio image was calculated from each filtered image pair. A uniform beam profile is not required because this technique is based on a ratio of two images, but spatial non-uniformity in the relative light collection efficiency between the two cameras must still be accounted for. This was achieved by dividing each ratio image by an average ratio image obtained in the gas-phase at room temperature.
To calibrate the ratio response with temperature for this specific detection setup, a thermocouple was positioned in the measurement plane during steady operation of the jet at different exit temperatures. The thermocouple readings were compared to mean intensity ratios obtained at the same location and a quadratic fit to this calibration data (Fig. 2) was used to convert the ratio images to temperature.

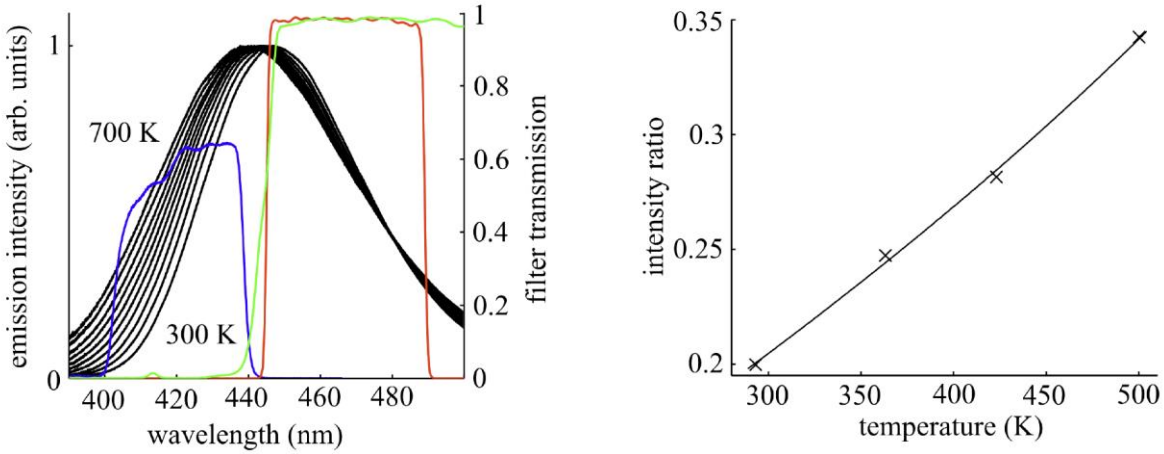

Fig. 2: Left: normalized BAM:Eu emission spectra, plotted at 50 K temperature intervals between 300 K and 700 K. The transmission curves of the beamsplitter (green) and the two filters (blue and red) used in this study are superimposed on the spectra. Right: intensity ratio response, measured in the gas phase.

For PIV, a dual-cavity, frequency doubled diode-pumped Nd:YAG laser was operated at 3 kHz with a pulse separation of 50 microseconds, equally bracketing the phosphorescence excitation light pulse. All lasers and cameras were triggered using a trigger clock and the start of the recording for the three cameras was synchronized via a custom-made manual trigger switch unit. The 532 nm laser beams were superimposed on the 355 nm beam using a dichroic mirror placed before the sheet optics, and the width of the 355 nm beam was adjusted with the telescope to match the thickness of the 532 nm sheets. For PIV, light scattered by the particles was imaged using a third CMOS camera (12 bit, 1024 x 1024 pixels) equipped with a Scheimpflug adapter, a 105 mm f/2.8 lens with the f-stop at f/11 and a 532-10 nm bandpass filter. The camera was operated at 6 kHz, with the pulse of each independently triggered laser cavity positioned at the respective end and start of consecutive frames. This results in double-frame acquisition at the desired 3 kHz. This camera was positioned on the opposite side of the measurement plane at a 6° angle to prevent any interfering background reflections between the two detection systems. Particle images were mapped to the phosphorescence images and then processed using a multi-pass cross-correlation algorithm with an interrogation window size of 32 x 32 and 50% overlap, resulting in a final vector spacing matching that of the temperature resolution (720 µm).

Results & Discussion

The architecture of CMOS cameras, where each pixel is read locally, can cause a number of issues related to nonlinearity and signal offset. These factors affect CMOS performance for quantitative diagnostics, and were previously investigated using a similar camera of an earlier generation (Weber et al. 2011). Nonlinearity was found to be less than 5% over the maximum dynamic range of the camera (12 bits) and the pixel-to-pixel variation in gain was within 1%. In this study, these effects were expected to have little impact on the temperature measurement as the recorded intensity after dark image subtraction was always below 500 counts, where the reported nonlinearity is below 2 %. To support this assumption, the effects of nonlinear sensor response on the measured ratio were experimentally investigated for the cameras used for thermometry. A phosphor pellet was placed behind two diffusive glass screens and illuminated by the laser at 100 Hz to prevent possible laser induced heating effects. As in later experiments, the cameras were allowed to thermally stabilize. Images of the phosphorescence emission were recorded using the two-camera system at a repetition rate of 3 kHz to exclude effects of different recording frequencies on camera performance. Different pulse energies of the laser were used to cover the range of phosphorescence signals encountered in the actual gas-phase measurements, with recorded intensities between 20 and 500 counts. Averages of 100 single shots were compiled for each illumination level to reduce the influence of statistical noise, and a homogenously illuminated region of 600 x 600 pixels was then extracted from each average ratio image. The ratio is 0.2 at room temperature (see Fig. 3), so nonlinearity will be indicated by differences between spatially averaged ratios obtained at different illumination levels, and pixel-to-pixel variations in gain will be manifested in spatial variations when dividing two average ratio images.
The spatially averaged ratio at each illumination level differed by less than 0.1%, indicating that in this intensity range the overall variation in camera gain is negligible. The pixel-to-pixel standard deviation of the divided average ratio images was 3.1%. Both findings are in good agreement with the previously mentioned study (Weber et al. 2011), when propagating the uncertainties for comparison with the divided ratio image evaluation used here. The spatial variation in pixel gain was reduced to 0.6% after the images were processed, so no image correction was performed in the actual gas-phase experiments.
The camera supplier provides an intensity calibration feature to correct for differences in pixel gain and dark levels based on an acquired dark image. This was disabled for this study since

it modifies the individual pixel gain after each calibration, which must be avoided for repeatability. Instead, a manual background subtraction was performed as described above.
Initial measurements also indicated frame-to-frame gain fluctuations across the entire chip causing frame-to-frame variation of the overall intensity ratio, which would ultimately result in an overall change in the mean measured temperature between frames. This effect was quantified using a stable tungsten light source placed behind a diffusive glass screen. Based on a homogeneously illuminated region comprised of 50 processed pixels in the centre of each intensity ratio image, the frame-to-frame standard deviation of the spatially averaged ratio was found to be 1.5%. This is larger than the single shot pixel-to-pixel standard deviation in the same area (0.7%), indicating these frame-to-frame fluctuations are an order of magnitude larger than the 0.01% expected when considering a statistical distribution of the sampled mean. To account for this effect in the present work, a region in the image at a known temperature was used to correct for frame-to-frame differences in the overall ratio. According to the manufacturer, the next generation of cameras features improved stability in the internal power supply, resulting in much smaller frame-to-frame gain fluctuations. This will decrease the measurement uncertainty caused by these fluctuations, which will eliminate the need for any correction procedure.
The single shot precision of the thermometry technique at 3 kHz was determined from imaging data recorded in the heated jet test case at four steady jet exit temperatures. Statistics based on 20,000 independent measurements taken from a region in the jet potential core show single shot pixel-to-pixel standard deviations of 4.9 K (1.7%), 7.8 K (2.2%), 9.2 K (2.2%) and 21.9 K (4.4%) at 293 K, 363 K, 423 K and 500 K, respectively. Signal statistics predict an error of 3.8 K at 293 K, indicating these results are close to the noise limit. From repeated measurement sequences, the maximum deviation of the mean measured temperatures to the flow temperature indicated by a thermocouple positioned in the measurement plane was only 5 K.
This level of temperature precision is comparable with that achieved in a previous study using a low speed measurement system based on interline transfer CCD cameras and low repetition rate flashlamp-pumped solid-state lasers (Fond et al. 2012). Because BAM:Eu saturates, the low pulse energy of the highspeed laser (around two orders of magnitude lower than the laser used previously) is not the limiting factor determining signal levels. The phosphorescence emission intensity is comparable for the two cases as saturation can also be achieved with the high-speed 355 nm laser. The readout noise of CMOS cameras is larger than that of the CCD cameras used previously. However, in this study this potential decrease in signal-to-noise ratio was compensated for by increasing the phosphorescence collection efficiency. The spectrally flat 50:50 beamsplitter used in the former study was replaced by a dichroic beamsplitter (Fig. 2), almost doubling the collection efficiency, and a filter with increased transmission and a larger passband was also used which increased the light level in one channel by an additional factor of four.
The pulse energy of the 355 nm laser is constant up to 10 kHz. Therefore, it should also be noted that the thermometry measurement could have been performed at frequencies up to 10 kHz (at reduced readout of 1024 x 744 pixels) without any decrease in the signal to noise ratio. In this experiment, the sampling rate for simultaneous measurements was limited by the PIV camera, which operated at nearly full frame readout to achieve comparable spatial resolution between the two measured fields.

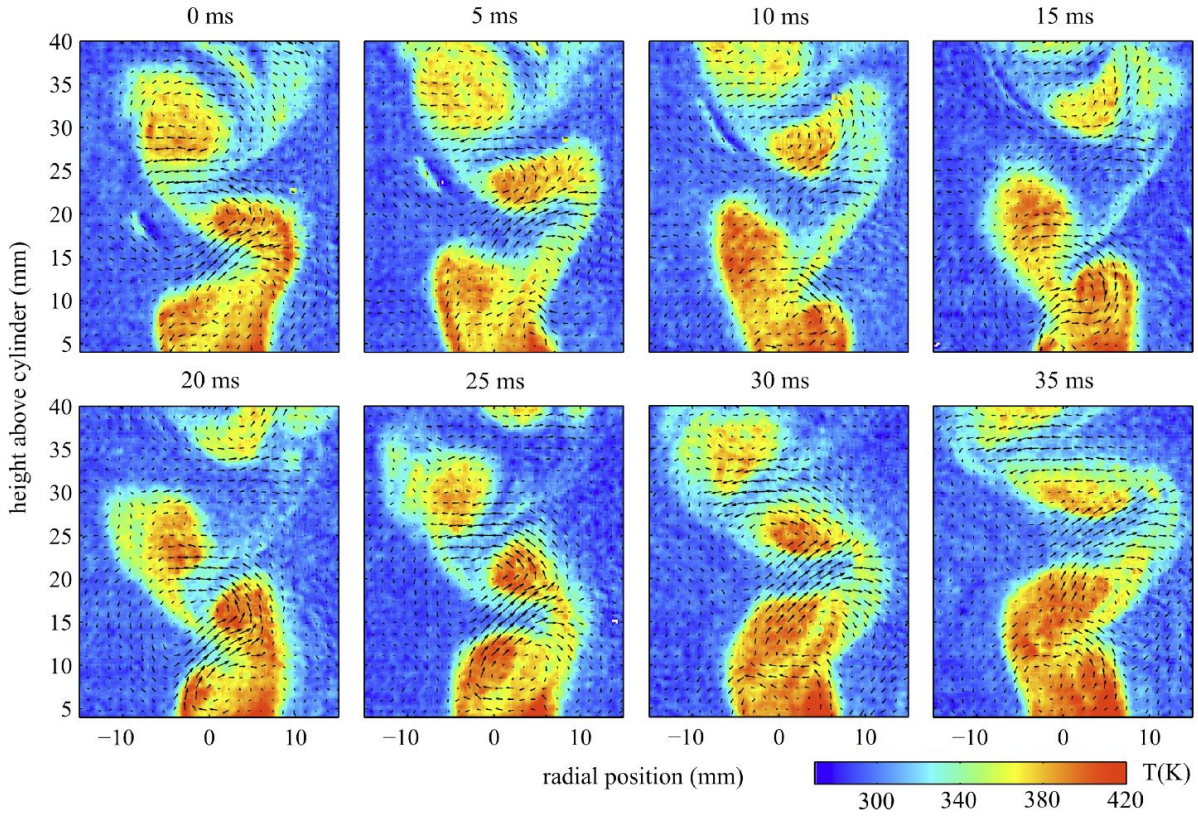

Fig. 3: Temporal evolution of the temperature and velocity fields in the wake of a heated cylinder. Every fifteenth image of the 3 kHz recording is displayed and the average velocity field is subtracted for better visualization of the eddies.

To demonstrate the utility of the combined diagnostics for the investigation of unsteady heat transfer phenomena, the time-resolved temperature and velocity fields were measured in the wake of the heated cylinder described earlier. Fig. 3 shows eight temperature and velocity fields, each separated by 5 ms. The mean velocity field has been subtracted from the instantaneous fields to better visualize the movement of eddies, and only every fifteenth image from the original 3 kHz recording is displayed so that the cyclic vortex shedding can be seen. Counter-rotating eddies of hot gas are alternately shed from either side of the rear stagnation point, which then cool as they are convected away from the cylinder.
The recording rate surpasses that required to resolve the phenomena of interest in this heat transfer study, but kHz rates are appropriate for the measurement of unsteady flow behavior more frequently encountered in the study of turbulent flows of practical interest. The 3 kHz rate was deliberately used to demonstrate the high image quality that can be obtained with these diagnostics. A video of this flow covering 50 ms at the full 3 kHz recording rate, allowing the visualisation of two full vortex shedding cycles, has also been published online (Abram et al. 2013).

Conclusions

Simultaneous planar measurements of gas temperature and velocity were demonstrated at sustained kHz repetition rates, using phosphor thermometry and a conventional PIV approach based on a single seeded tracer. The setup requires high-speed solid-state lasers only and non-intensified high-speed cameras, similar to conventional kHz PIV systems. The CMOS cameras were characterized for ratio-based imaging and shown to be suitable for quantitative measurements. The use of a fast, high quantum yield phosphor tracer permits precise temperature measurements at kHz rates in an oxygen containing environment, de-

spite the low pulse energy of the high-speed 355 nm laser. The study demonstrates the potential of this technique for time-resolved investigations of unsteady heat transfer phenomena.

References

Abram C, Fond B, Heyes AL, Beyrau F (2013) “High-speed planar thermometry and velocimetry using thermographic phosphor particles”, Appl. Phys. B **111**, 155-160

Fond B, Abram C, Heyes AL, Kempf AM, Beyrau F (2012) “Simultaneous temperature, mixture fraction and velocity imaging in turbulent flows using thermographic phosphor tracer particles”, Opt. Express **20**, 22118-22133

Fond B, Abram C and Beyrau (2015) “On the characterisation of tracer particles for thermographic particle image velocimetry”, Appl. Phys. B **118**, 393-399

Jenkins TP, Wu F, Turner KI (2012) “On the development of flow thermometry imaging for high temperature using thermographic phosphors”, 50th AIAA Aerospace Sciences Meeting

Jordan J, Rothamer DA (2013) “Pr:YAG temperature imaging in gas-phase flows”, Appl. Phys. B **110**, 285-291

Klein PH and Croft WJ, “Thermal conductivity, diffusivity, and expansion of Y_2O_3, $Y_3Al_5O_{12}$, and LaF_3 in the range 77 K–300 K”, J. Appl. Phys. **38**, 1603 (1967)

Omrane A, Petersson P, Aldén M, Linne MA (2008) “Simultaneous 2D flow velocity and gas temperature measurements using thermographic phosphors”, Appl. Phys. B **92**, 99–102

Picano F, Battista F, Troiani G, and Casciola CM, “Dynamics of PIV seeding particles in turbulent premixed flames”, Exp. Fluids **50**, 75–88 (2011)

Raffel M, Willert C, Wereley C, and Kompenhans J, “Particle Image Velocimetry: A Practical Guide”, 2nd ed. (Springer, 2007)

Rothamer DA, Jordan J (2012) “Planar imaging thermometry in gaseous flows using upconversion excitation of thermographic phosphors”, Appl. Phys. B **106**, 435–444

Weber V, Brübach J, Gordon RL, Dreizler A (2011) “Pixel-based characterisation of CMOS high-speed camera systems”, Appl. Phys. B **103**, 421-433

Williamson CHK (1996) “Three-dimensional vortex dynamics in bluff body wakes”, Annu. Rev. Fluid Mech. **28**, 477-539